Journal of ELECTRONIC MATERIALS, Vol. 45, No. 12, 2016
DOI: 10.1007/s11664-016-4908-4

Effect of Plasma Surface Finish on Wettability and Mechanical Properties of SAC305 Solder Joints

KYOUNG-HO KIM,[1,2] JUNICHI KOIKE,[2] JEONG-WON YOON,[1,3,4] and SEHOON YOO[1,3,5]

1.—Welding and Joining R&D Group, Korea Institute of Industrial Technology (KITECH), 156 Gaetbeol-ro, Yeonsu-gu, Incheon 21999, Korea. 2.—Department of Materials Science, Tohoku University, 6-6-11 Aoba, Aramaki, Aoba-ku, Sendai 980-8579, Japan. 3.—Critical Materials and Semiconductor Packaging Engineering, University of Science and Technology (UST), 217 Gajeong-ro, Yuseong-gu, Daejeon 34113, Korea. 4.—e-mail: jwyoon@kitech.re.kr. 5.—e-mail: yoos@kitech.re.kr

The wetting behavior, interfacial reactions, and mechanical reliability of Sn-Ag-Cu solder on a plasma-coated printed circuit board (PCB) substrate were evaluated under multiple heat-treatments. Conventional organic solderability preservative (OSP) finished PCBs were used as a reference. The plasma process created a dense and highly cross-linked polymer coating on the Cu substrates. The plasma finished samples had higher wetting forces and shorter zero-cross times than those with OSP surface finish. The OSP sample was degraded after sequential multiple heat treatments and reflow processes, whereas the solderability of the plasma finished sample was retained after multiple heat treatments. After the soldering process, similar microstructures were observed at the interfaces of the two solder joints, where the development of intermetallic compounds was observed. From ball shear tests, it was found that the shear force for the plasma substrate was consistently higher than that for the OSP substrate. Deterioration of the OSP surface finish was observed after multiple heat treatments. Overall, the plasma surface finish was superior to the conventional OSP finish with respect to wettability and joint reliability, indicating that it is a suitable material for the fabrication of complex electronic devices.

Key words: Plasma surface finish, Pb-free solder, Sn-3.0Ag-0.5Cu, wettability, mechanical properties

INTRODUCTION

The soldering process and reliability of the joints between the components highly depend on the quality of the surface finish of a printed circuit board (PCB).[1–3] To ensure high quality solder interconnects, the PCB surface finish should have a high solderability, low process cost, low thermal stress, and long shelf life. In addition, the thickness of the intermetallic compound (IMC), composition, microstructure, mechanical properties, and reliability of solder joints are strongly dependent on the surface finish layers.[3–5] Among conventional surface finishes, such as organic solderability preservative (OSP), immersion tin, immersion silver, and electroless nickel immersion gold, OSP is the most common as it has simple processing, low cost, environmentally friendliness, and adequate solderability.[6–11] However, the OSP surface finish has several disadvantages, such as a short shelf life, low corrosion resistance, and weak multiple soldering property.[5,12] In particular, the latter is one of the most important parameters for the high quality assembly of complicated electronic modules.[13,14] For example, double-sided PCBs are subjected to at least two reflow processes (i.e., heat treatments). During this procedure, the bottom side of the double-sided PCB is exposed to high temperature under an air atmosphere. If wave soldering and

(Received April 15, 2016; accepted August 25, 2016; published online September 6, 2016)

rework processes are used for the assembly of the electronic module, at least four heat treatments are required. Therefore, the surface finishes that are not soldered at each step of the process can be degraded by the oxidizing environment during heating. For these reasons, a PCB surface finish with high stability during multiple soldering steps is essential to ensure the reliability of solder joints.

The plasma surface finish is a thin and protective coating that is a potential replacement for the conventional surface finishes with several advantages. The shelf life of the plasma finished PCB is over 1 year, and the corrosion resistance of the plasma finish layer is generally higher than those of the conventional surface finishes.[15] The plasma surface finish is more environmentally friendly than the wet chemical processes currently used, as it eliminates the use of water, precious and semi-precious metals including gold, palladium, and nickel, and is a safer process for operators.[15] Nevertheless, detailed studies regarding the reliability of the plasma finish and comparisons of the plasma and OSP finishes remain insufficient. Therefore, in this study, we investigate the effects of multiple heat treatments on the solderability (or wettability) of plasma and OSP finished Cu coupons using a wetting balance test with Sn-3.0Ag-0.5Cu (SAC305) solder. In addition, we formed SAC305 solder ball on the two different PCB substrates and investigated the interfacial reactions and mechanical shear properties of solder joints formed during sequential heat treatments and reflow processes. The relationships between solderability, interfacial reaction, and shear force applied to the solder joints are discussed.

EXPERIMENTAL

The PCBs used in this study were solder mask defined (SMD) flame retardant 4 (FR-4) type. A schematic of the test PCBs is shown in Fig. 1. The diameter of the Cu pads on the PCB was 400 μm, and the thicknesses of the Cu pads and photo solder resist (PSR) were 10 μm and 15 μm, respectively. For the plasma surface finish, an organic thin film was deposited onto the Cu pad of the test PCB using plasma-enhanced chemical vapor deposition (PE-CVD) (JESAGI Hankook Corp. Korea). The precursor used in the plasma coating process was fluorocarbon. Conventional OSP finished PCBs were also used in this study as a reference for comparing the quality of the plasma surface finish. The microstructures of the plasma and OSP finished layers were analyzed using transmission electron microscopy (TEM, JEOL JEM 4010).

To understand the effects of the plasma and OSP surface finishes on the solder wetting properties, Cu wetting test coupons with dimensions of 1.0 × 3.0 × 0.3 mm^3 were prepared. The solderability of the two surface finishes was measured by a wetting balance tester (MALCOM, SP2). A

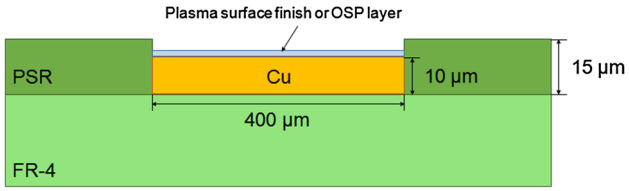

Fig. 1. Schematic illustration of the test samples used in this study, showing the FR-4 PCB, photo solder resist (PSR), the Cu pads, and the surface finish layers.

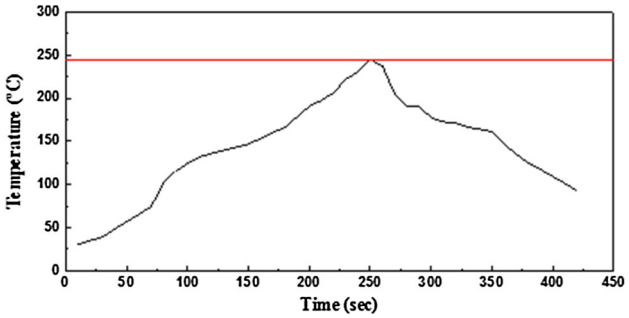

Fig. 2. Temperature versus time reflow profile for the Sn-3.0Ag-0.5Cu solder.

SAC305 solder was used in the wetting test. The wetting temperature was 250°C, and the sample immersion speed, depth, and time were 5 mm/s, 5 mm, and 10 s, respectively. Ten measurements were made at each test condition in order to improve the statistical confidence level of the results. The maximum wetting force (F_{max}) and zero-cross time (T_{zero}), were used to assess the wetting behavior of the surface finishes. To simulate the effect of the multiple heat treatments on the solderability of the two surface finishes, the test coupons were heat treated in a reflow oven (Heller, 1890UL) under typical SAC305 reflow conditions (as described by the heating profile shown in Fig. 2). The peak temperature of the reflow profile was approximately 242°C. The wetting tests were performed after the samples had experienced either zero, two, or four heat treatments. In the solder spreading test, SAC305 solder paste was screen-printed on the OSP and plasma finished PCBs, and then the PCBs were reflowed. The diameters of the printed solder paste and Cu pads on the PCB were 300 μm and 400 μm, respectively. Optical microscopy (OM) was used to observe the surfaces of the PCBs after testing. The spreading areas were measured using image analysis software and the spreading ratios were calculated as the increase in area as a percentage.

Soldering was performed in order to evaluate the interfacial reactions and mechanical strength of the joints between the SAC305 solder alloy and the two different surface finishes. Firstly, SAC305 solder paste (Senju, M705-SHF type 5) was printed on the test PCB (Fig. 1) using a stencil mask. Secondly,

SAC305 solder balls (Duksan Hi-Metal, Korea) with a diameter of 450 μm were placed on the printed SAC305 solder paste. Then, the test PCB was heated in a reflow oven (Heller, 1890UL) using the temperature profile shown in Fig. 2. To investigate the solderability of the surface finishes, the test PCBs were heat treated various times in the reflow oven under the same conditions. After multiple heat treatments, solder paste and balls were applied to the test PCBs and reflowed to form solder joints. The multiple heat treatments were performed up to four times. For example, samples heat treated two times were subjected to two heat treatments without soldering, and finally, the reflow process with the solder alloy. After the reflow processes, the samples were prepared for observation of the interface cross-sections. Common metallographic practices, grinding and polishing, were used to prepare the samples. The microstructures and chemical compositions were analyzed using field emission scanning electron microscopy (FE-SEM, FEI Inspect F) and TEM equipped with an energy dispersive x-ray spectroscopy system (EDS).

Ball shear tests were performed on the reflow samples using a shear tester (DAGE 4000) with a shear tool height of 50 μm and a shear speed of 300 μm/s. The average shear strength of 20 solder balls, after the minimum and maximum outlier values had been removed, was recorded. After the ball shear testing, the fracture surfaces were investigated thoroughly using SEM and EDS.

RESULTS AND DISCUSSION

Good wetting properties are very important for solder alloys to ensure a reliable connection between the solder and the components. The solderability of the SAC305 alloy with different surface finishes was measured using a wetting balance test. This alloy system is technically important because it is generally recognized as the first choice for a Pb-free solder.[4] Figure 3 shows the wetting force and zero-cross time as a function of the number of heat treatments for the different surface finishes. For each surface finish, F_{max} and T_{zero} were calculated by averaging 10 sets of wetting data (where the error bars represent the standard deviation of these data sets). In the case of the plasma surface finish, the wetting force did not change with increasing numbers of heat treatments. On the other hand, the wetting force of the OSP surface finish rapidly decreased with further heat treatments. The zero-cross times for both surface finishes increased with increasing number of heat treatments. However, the zero-cross time of the OSP finish increased more rapidly than that of the plasma finish. The plasma finished samples had higher wetting forces and shorter zero-cross times than the OSP surface finish.

Figure 4 shows OM images of the test coupons after the wetting tests, where 0, 2, and 4 refer to the number of heat treatment cycles before wetting. Interesting results were observed for the OSP samples. In the case of the sample heat treated four times, the wetting reaction did not occur, as shown in Fig. 4a. On the other hand, the wetting reactions occurred for the plasma samples irrespective of the number of heat treatments, as shown in Fig. 4b. These results are consistent with the wetting test results shown in Fig. 3. These results indicate that the OSP surface finish was degraded after multiple heat treatments. Similar results are reported in the literature.[15,16] It has been reported that the solderability of the OSP finish reduced after two reflow

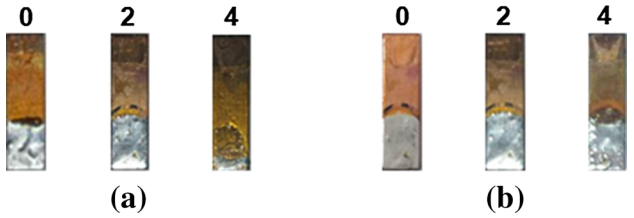

Fig. 4. OM images of the test coupons after wetting tests; (a) OSP and (b) plasma surface finishes subjected to 0, 2, or 4 heat treatment cycles before wetting.

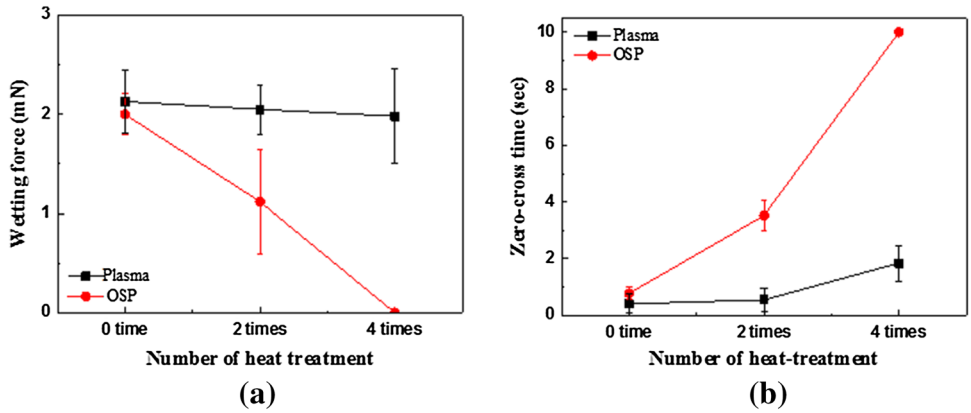

Fig. 3. Wetting test results for the plasma and OSP surface finishes as a function of heat treatment cycles; (a) wetting force and (b) zero cross time.

cycles. On the other hand, we have demonstrated that the solderability of plasma finished PCBs was still high after multiple heat cycles, making it suitable for the fabrication of complex electronic devices.

Figure 5 shows OM images of the spreading test samples for 0, 2, and 4 heat treatment cycles, along with a schematic diagram illustrating the reflow process for both the OSP and plasma finished PCBs. The percentages refer to the spreading ratios. In the case of the plasma finished sample, the initial spread ratio was around 120%, which dropped slightly to around 115% after reflowing. The spread ratio of the initial OSP finished sample was similar to that of the plasma finished sample, but decreased to around 108% after two heat treatment cycles and further to 77% after four heat treatments. These results are consistent with the observations of the wetting tests shown in Fig. 3.

The morphologies of the OSP and plasma finished PCB substrates were analyzed using TEM. Figure 6 shows cross-sectional TEM images of the OSP and plasma surface finished Cu substrates. The Cu substrates are the bulk region of the right hand sides of the images and the white layers are the surface coating films. The Au, Pt, and carbon layers indicated on the images were deposited as protection layers for the TEM sample preparation. In addition, the thicknesses of the OSP and plasma coated layers are indicated with red arrows in Fig. 6. The thickness of OSP layer ranged from 40 to 60 nm. On the other hand, the plasma coated layer had about 20 nm-thick. The plasma coating process involved plasma polymerization, the formation of polymeric materials under the influence of plasma conditions,[17] which allows the deposition of continuous organic films from the gas phase on a metal substrate. The plasma process creates a dense and highly cross-linked polymer coating on metal substrates.

In order to evaluate the effect of the surface finish on the soldering and interfacial reactions, a reflow process was conducted using the SAC305 solder. Figure 7 shows the cross-sectional TEM images for the OSP and plasma samples after soldering. The plasma surface finish was applied across the whole of the PCB and was removed by the soldering process only in the areas where flux and solder were applied. In this study, the plasma coated layer was removed by the combined action of the flux and the high reflow temperature used during the reflow process. As a result, the Cu layer beneath the plasma coated layer was then in direct contact with the molten solder, resulting in the formation of Cu-Sn IMCs at the interface. The interfacial reactions and IMC formation in this solder system are well-known and have been reported in previous studies.[18,19] During the reflow process, the SAC305 solder was in the molten state and typical scallop-shaped Cu_6Sn_5 IMCs formed at the interfaces. In addition, thin Cu_3Sn layers were observed between the Cu_6Sn_5 IMC and the Cu substrate. Most Sn-based solder alloys form these two reaction layers (Cu_6Sn_5 and Cu_3Sn) at the interface between the solder and Cu substrate. Consequently, similar interfacial structures were observed at the interfaces of the solder joints for both samples.

Figure 8 shows cross-sectional SEM images of the SAC305 solder joints with the two surface finishes after sequential heat treatments and reflow process. From the TEM results shown in Fig. 7, we confirmed that Cu_6Sn_5 and Cu_3Sn formed as reaction products at the interfaces. A close examination of the cross-sectional SEM images revealed that the thicknesses of the interfacial IMCs for the two surface finishes were similar (as shown in Fig. 9).

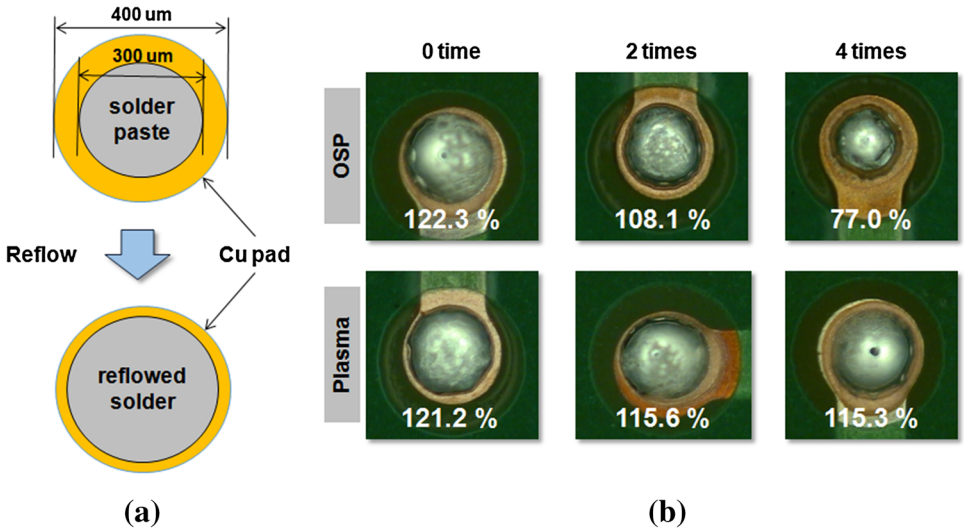

Fig. 5. (a) Schematic illustration of the solder spreadability test and (b) OM images of the soldered PCBs after spreading tests for OSP and plasma surface finished samples subjected to multiple heat treatments.

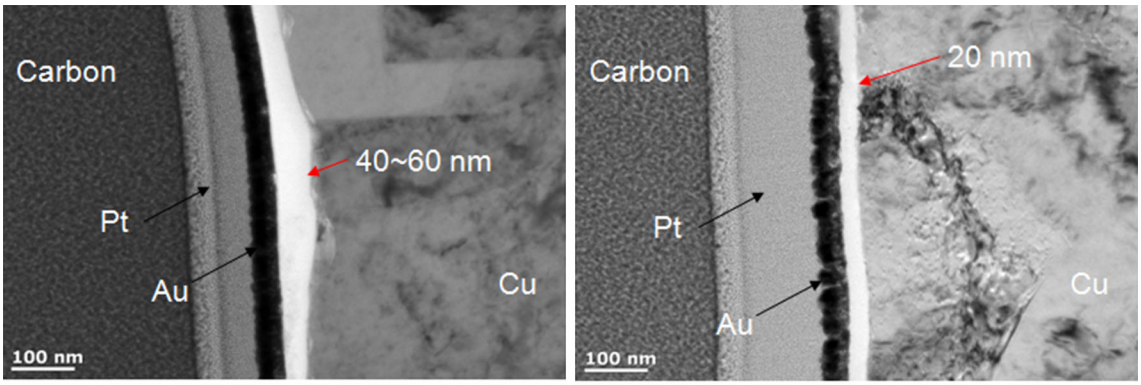

Fig. 6. Cross-sectional TEM micrographs of the (a) OSP and (b) plasma surface finished Cu substrates, where the surface finish layers are the white film.

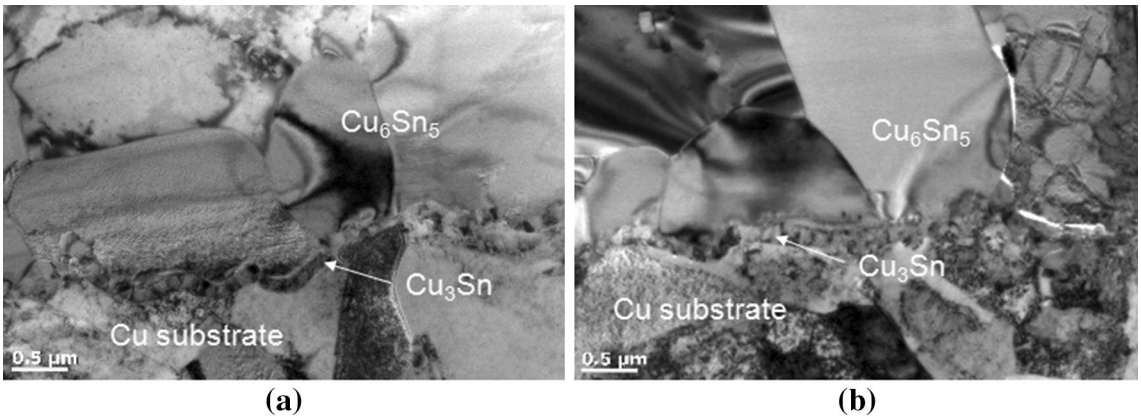

Fig. 7. Cross-sectional TEM images after soldering of the (a) OSP and (b) plasma surface finished samples showing the formation of IMC grains.

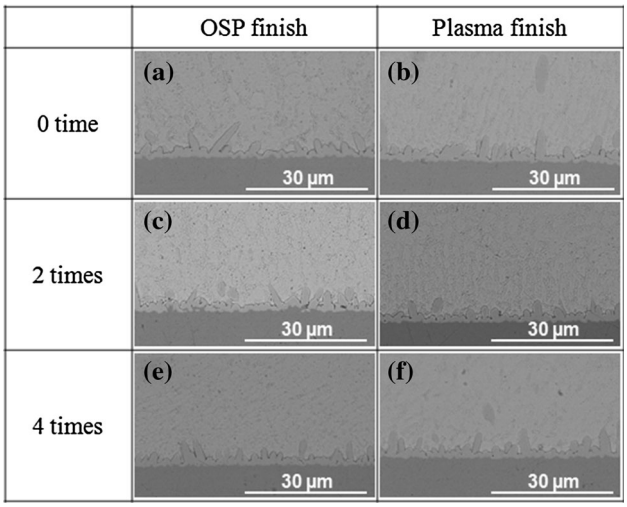

Fig. 8. Cross-sectional SEM micrographs of the SAC305 solder joints with different surface finishes after sequential heat treatments and reflow process.

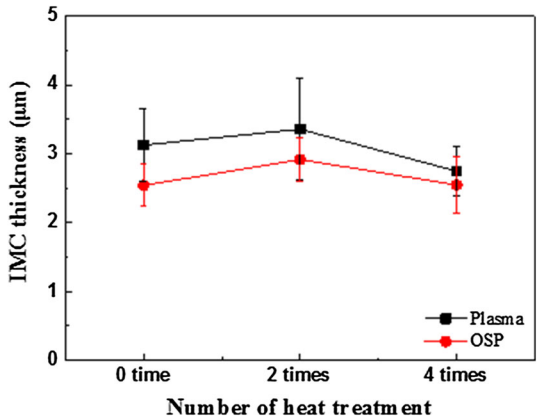

Fig. 9. Average thicknesses of the IMC layers within the SAC305 solder joints with different surface finishes after sequential heat treatments and reflow process.

Figure 10 shows the results of the ball shear tests performed to evaluate the effect of the surface finish and interfacial reactions on the mechanical reliability of the SAC305 solder joints as a function of multiple heat treatments. As mentioned before, the solder reflow tests were performed after the samples had experienced either zero, two, or four heat treatments. In the case of the plasma coating,

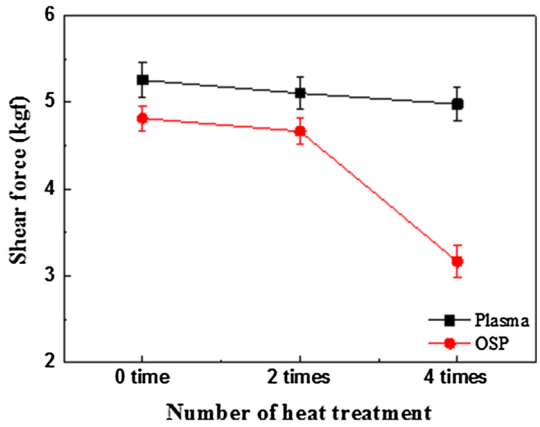

Fig. 10. Average shear force of the SAC305 solder joints with different surface finishes after sequential heat treatments and reflow process.

the shear force remained nearly constant at approximately 5.2 kgf despite multiple reflows. On the other hand, the shear force decreased rapidly after four heat treatments for the OSP substrate. The shear force for the OSP joint without heat treatment was approximately 4.7 kgf, dropped a little after two heat treatments, and finally decreased dramatically to a shear force of 3.2 kgf after four heat treatments. Overall, the shear force for the plasma substrate was consistently higher than that for the OSP substrate. As the shear force is related to the force required to fracture the solder joint, a high value indicates a stronger joint.

Figure 11 shows cross-sectional SEM images of the entire SAC305 solder joints with different surface finishes and heat treatment cycles. In the case of the plasma substrate, the SAC305 solder alloy covered all of the Cu pad area (indicated by the white dashed line), even after multiple heat treatments. On the other hand, for the OSP substrate the SAC305 solder did not perfectly cover (i.e., react with) the Cu pads. This was due to the deterioration of the OSP surface finish after multiple heat treatments. The un-reacted parts of the Cu are indicated by the white arrows in Fig. 11c and e. These results are consistent with those from the wetting tests shown in Figs. 3, 4, and 5.

Another interesting observation of this study was that voids formed at the OSP/solder interfaces after multiple heat treatments (although not at the plasma finished interface). These voids are indicated by the black arrows in Fig. 11. Yoon et al. studied the relationship between the interfacial reactions, void formation, and mechanical reliability of SAC305/OSP-finished Cu joints.[19] In that study, several voids formed at the interface of the OSP-finished Cu joint subjected to a temperature-humidity test. The voids were caused by the oxidation of the OSP finished Cu substrate during testing. Shear tests were also performed and it was found that the mechanical reliability of the solder joint

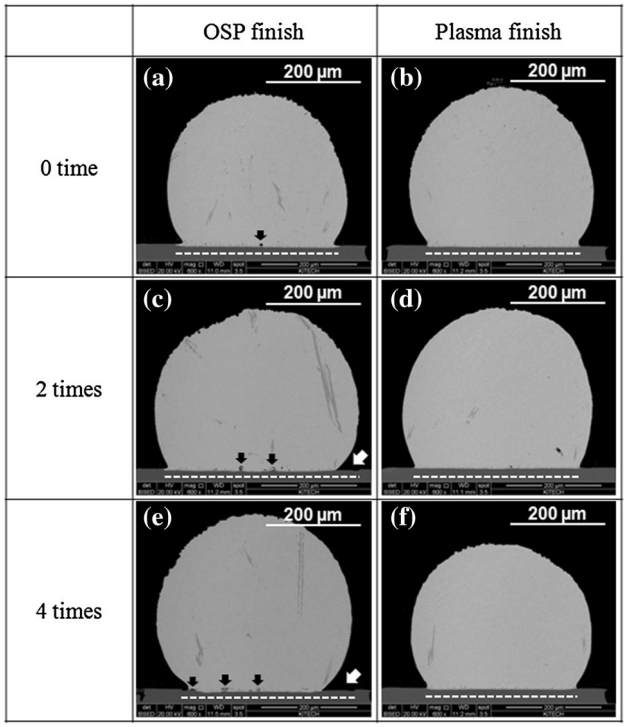

Fig. 11. Cross-sectional SEM micrographs of the SAC305 solder joints with different surface finishes after sequential heat treatments and reflow process. The white dashed lines indicate the Cu pad, the white arrows indicate the unreacted area of the Cu pad, and the black arrows indicate voids developed at the interfaces.

was degraded by these voids at the interface. It is interesting to note that the formation of the Cu_6Sn_5 IMC in the SAC305 solder matrix was significantly retarded for the SAC305/plasma finish joint, compared with the SAC305/OSP finish system where several relatively large Cu_6Sn_5 IMCs were observed in the OSP joints, as shown in Fig. 11a, c, and e.

The fracture surfaces after ball shear testing were examined using SEM in order to verify the variations in the shear force. Figure 12 shows the fracture surfaces of the two types of SAC305 solder joints with different surface finishes and multiple heat treatments. The direction of the shear is indicated by the black arrow in Fig. 12. From these fracture surfaces we can conclude that the failure mode was consistently related to the bulk for the plasma-finished substrate, regardless of the number of heat treatment cycles. Similarly, in the case of the OSP-finished substrate, bulk solder failures were observed for the samples subjected to zero and two heat treatments. However, a significantly different fracture surface was observed for the SAC305/OSP joint after four heat treatment cycles, where there were many voids observed at the interface. In addition, the shearing area decreased significantly for the OSP joint heat-treated four times. In Fig. 12c we have indicated the area of the Cu pad with a white dashed circle and the area un-reacted Cu is shown by the white arrow. The results shown

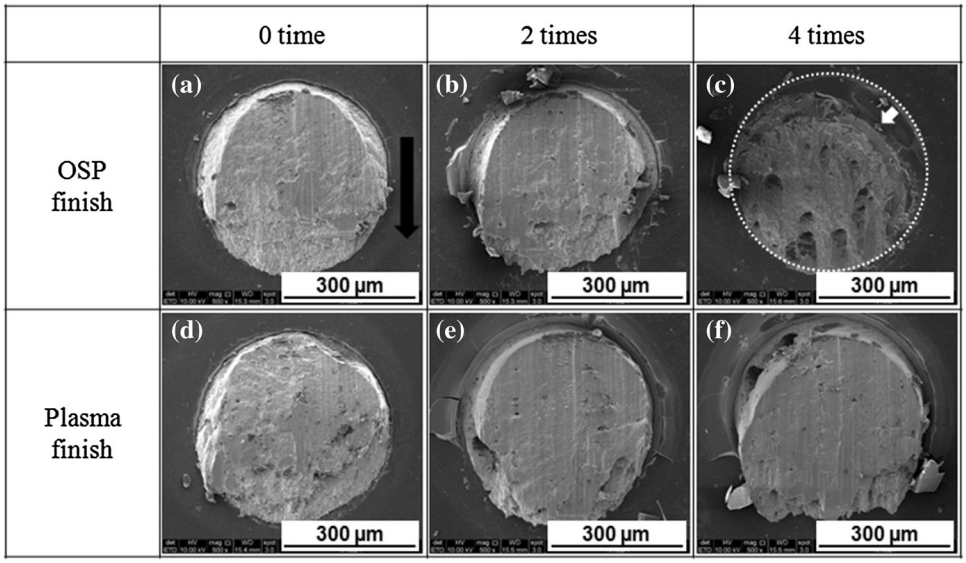

Fig. 12. SEM micrographs of the fracture surfaces of the solder joints after shear testing. The white dashed circle indicates the area of the Cu pad, the white arrows indicates the unreacted area with the Cu pad, and the black arrow indicates the direction of shear.

in Fig. 12 are consistent with those of the interfacial microstructures from the cross-sectional SEM micrographs shown in Fig. 11. From the wetting test results in Figs. 3, 4, and 5, we confirmed that the OSP surface finish was degraded after multiple heat treatments. The un-reacted parts of the Cu in Figs. 11 and 12 are caused by the poor wetting property and deterioration of the OSP coating layer after multiple heat treatments. In conclusion, the reduced bonding area and void formation resulted in the abrupt decrease of the shear force in the OSP joint after multiple heat treatments.

CONCLUSION

In this study, the effects of multiple heat treatments on the wettability, interfacial reactions, and mechanical reliability of SAC305 solder on plasma surface finished PCBs were investigated, and the results compared to those for the SAC305/OSP system.

Wetting and spreading tests showed that the plasma finished samples had higher wetting forces and shorter zero-cross times than the OSP surface finish. The wetting force (and hence solderability) was not dependent on the number of heat treatment for the plasma surface finish, whereas the wetting force rapidly decreased with further heat treatments for the OSP surface finish. In the case of the multiple heat-treated OSP sample, the wetting reaction did not occur due to the degradation of the OSP.

The plasma coated layer was uniformly formed on the Cu pad with a thickness of about 20 nm. This layer was removed by the combined action of the flux and the high reflow temperature used during the reflow process. This resulted in the Cu layer coming into direct contact with the molten solder, resulting in the formation of Cu-Sn IMCs at the interface. In the reflow reaction with SAC305 solder, the morphology and thickness of the interfacial IMCs for the two surface finishes were similar.

From ball shear tests it was found that the shear force for the plasma substrate was consistently higher than that for the OSP substrate. In the case of the plasma substrate, the shear force was independent of the number of heat treatments, while it decreased rapidly after four heat treatment cycles for the OSP substrate. The poor wettability, reduced bonding area, and void formation of the OSP finish after multiple heat treatments resulted in degradation of the joint.

These results clearly indicated that the plasma surface finish was superior to the conventional OSP finish with respect to wettability and joint reliability.

ACKNOWLEDGEMENTS

This work was financially supported by a research project from the Ministry of Trade, Industry and Energy, Republic of Korea.

REFERENCES

1. M. Abtew and G. Selvaduary, *Mater. Sci. Eng. R* 27, 95 (2000).
2. C.M.L. Wu, D.Q. Yu, C.M.T. Law, and L. Wang, *Mater. Sci. Eng. R* 44, 1 (2004).
3. T. Laurila, V. Vuorinen, and J.K. Kivilahti, *Mater. Sci. Eng. R* 49, 1 (2005).
4. J.W. Yoon, B.I. Noh, and S.B. Jung, *J. Electron. Mater.* 40, 1950 (2011).
5. T.H. Wang, C.H. Tsai, and Y.S. Lai, *Microelectron. Eng.* 98, 1 (2012).
6. D. Chang, F. Bai, Y.P. Wang, and C.S. Hsiao, in *6th Electronics Packaging Technology Conference (EPTC)* (2004), pp. 149–153.

7. Y.D. Jeon, Y.B. Lee, and Y.S. Choi, in *56th Electronic Components and Technology Conference (ECTC)* (2006), pp. 119–124.
8. Y. Kim, J.W. Shin, and K.W. Paik, in *64th Electronic Components and Technology Conference (ECTC)* (2014), pp. 1765–1768.
9. W. Wang, A. Choubey, M.H. Azarian, and P.M. Pecht, *J. Electron. Mater.* 38, 815 (2009).
10. W.H. Zhu, L. Xu, J.H. Pang, X.R. Zhang, E. Poh, Y.F. Sun, A.Y.S. Sun, C.K. Wang, and T.B. Tan, in *58th Electronic Components and Technology Conference (ECTC)* (2008), pp. 1667–1672.
11. T.K. Lee, H. Ma, K.C. Liu, and J. Xue, *J. Electron. Mater.* 39, 2564 (2010).
12. C.K. Chung, Y.J. Chen, C.C. Li, and C.R. Kao, *Thin Solid Films* 520, 5346 (2012).
13. P. Liu, P. Yao, and J. Liu, *J. Alloys Compd.* 470, 188 (2009).
14. Y.S. Lai, J.M. Song, H.C. Chang, and Y.T. Chiu, *J. Electron. Mater.* 37, 201 (2008).
15. F. Ferdinandi, in *International Conference on Surface Mount Technology Association (SMTA)* (2009), pp. 841–846.
16. D.A. Geiger, Y. Liu, and D. Shangguan, in *International Conference on Surface Mount Technology Association (SMTA)* (2005), pp. 1–5.
17. A. Brooks, S. Woollard, G. Hennighan, and T. von Werne, in *International Conference on Surface Mount Technology Association (SMTA)* (2012), pp. 1–6.
18. B.S.S.C. Rao, J. Weng, L. Shen, T.K. Lee, and K.Y. Zeng, *Microelectron. Eng.* 87, 2416 (2010).
19. J.W. Yoon, B.I. Noh, Y.H. Lee, H.S. Lee, and S.B. Jung, *Microelectron. Reliab.* 48, 1864 (2008).